

HYDRATE CELLULOSE FILMS AND PREPARATION OF SAMPLES  
 MODIFIED WITH NICKEL NANO- AND MICROPARTICLES.  
 II. INTERCALATION OF NICKEL INTO HYDRATE CELLULOSE FILMS

NINA E. KOTELNIKOVA and ALEXANDRA M. MIKHAILIDI\*

*Institute of Macromolecular Compounds, Russian Academy of Sciences,  
 St. Petersburg, Russia*

*\*Saint-Petersburg State University of Technology and Design, St. Petersburg, Russia*

Received March 22, 2011

Nanocomposite materials containing stabilized nickel nano- and microparticles in the matrix of the hydrate cellulose film (HCF) have been prepared. Ni nanoparticles were synthesized directly in the film, by the diffusion-reduction method. The efficiency of reducers on the chemical reduction of nickel ions has been compared. The crystalline structure of the HCF-Ni samples was analyzed by X-ray diffraction, and their morphology was studied by SEM analysis. The structure of the cellulose remained unchanged was compared to the pristine one. Particle sizes, dependent on the reducer type, were measured in nanometers, according to the micrometer scale.

**Keywords:** hydrate cellulose film, nickel nano- and microparticles, X-ray diffraction, SEM analysis

## INTRODUCTION

The study of compounds in a nanocrystal state permits the preparation of functional materials with desired physico-chemical characteristics.<sup>1</sup> Many properties of the substances are essentially changed, when they are converted into nanoscale materials. For example, the electronic and magnetic properties of nanoscale substances differ appreciably from those of bulky materials. In recent years,<sup>2-8</sup> numerous polymer nanocomposites containing stabilized nanoparticles of metals – namely, silver, copper, nickel, platinum and palladium – have been synthesized. The presence of metal nanoparticles in polymers imparts electrical, magnetic, and catalytic properties to polymer nanocomposites.<sup>9</sup>

The synthesis of nickel nanoparticles has been intensely studied,<sup>10</sup> since the preparation of nickel coatings in the 1960s, due to the possibility to prepare magnetic materials and catalysts. In the monographs and papers published<sup>11-13</sup> in the 1980s, the chemical reduction of a number of metals, including

nickel, in polymer matrices, such as PE, PP, PET, PVC, PVA, PAA and PVP, was described. For instance, composites containing up to 20 vol% nickel in the PP bulk were prepared. In these cases, zero-valent metals occurred in a finely dispersed state. The study of the zero-valent copper and nickel particles formed in aqueous solutions of PVP, poly(ethylene glycol), poly(*N*-vinylcaprolactam) and in the interpolymer complex of poly(acrylic acid) with (urea–formaldehyde) polymer showed that small metal particles, 3-15 nm in diameter and with narrow size distribution, were united into spherical flocks, 30-140 nm in diameter, and occurred in the resulting suspensions.<sup>14-15</sup> The synthesis of these nanocomposites *via* the reduction of metal ions in the solutions of the above polymers is based on the formation of a stable metal particle–macromolecular complex.<sup>16</sup>

The properties of nanoparticles in the bulk of polymer matrices determine the properties of nanocomposites as a whole. The most important of them are the following:

nanoparticle size, shape, size distribution and stability to oxidation. In most cases, the nanoparticles are prepared in the solutions or gels of synthetic polymers. Since the stabilization of nanoparticles with the simultaneous control of their size and shape remains an unsolved problem, the use of solid ordered matrices, the so-called nanoreactors, has attracted considerable interest in recent years. Unlike in polymer solutions, a marked aggregation of nanoparticles may be avoided in this case.<sup>1,17</sup> For the synthesis of nanoparticles in the solid matrix of the synthetic polymers, they should possess a well-developed porous system. To improve the system, the methods of polymer stretching in active liquid media are usually employed.<sup>11</sup>

The use of high surface nanoreactors and of the initially existing system of pores is of special interest. Cellulose, a highly porous fibre material (pore size ranging between 1-10  $\mu\text{m}$ ) with a high specific area, is one of them. Therefore, it has been employed to intercalate nanoparticles of transition metals, such as silver, platinum, palladium and copper without any additional treatment of cellulose.<sup>18-20</sup> Data on the synthesis of Ni nanoparticles in the cellulose matrix are scarce. The preparation of disperse nanoparticles of nickel and of its oxides (with sizes of 5-21  $\mu\text{m}$ ) *via* the thermal decomposition of cellulose-hydrous nickel gel membrane has been described.<sup>21</sup> The nickel nanoparticles have been successfully intercalated into the matrix of microcrystalline cellulose.<sup>22</sup> An additional advantage of applying cellulose as a matrix for metal nanoparticles is its biodegradability and harmlessness to both humans and animals.

In a previous paper,<sup>23</sup> the physico-chemical properties of a hydrate cellulose film (HCF) have been described, and its morphological and structural characteristics have been analyzed with IR Fourier transform spectroscopy, <sup>13</sup>C NMR spectroscopy, X-ray photoelectron spectroscopy, WAXS and SEM.

The use of HCF in nanotechnological processes has been poorly described so far. This particularly applies to processes of metal species intercalation into HCF. Thorough investigations were devoted to obtaining new materials for new applications, and to the study of their properties.<sup>24,25</sup> Several examples describing the preparation of packaging HCFs containing various additives, including nanoparticles of silver or titanium dioxide with

bactericidal properties, have been discussed in patents and papers.<sup>26-28</sup> The process of film obtaining was mainly accomplished by the embedding of ready-made nanoparticles into the reaction mixture during film formation. HCF was first used as a basis for nanocomposites with intercalated silver nanoparticles, occurring in the form of clusters or aggregates.<sup>29</sup> Silver nanoparticles were embedded into the matrix by the reduction of silver ions to silver (0) directly in the film matrix. Tests on the antimicrobial activity of HCFs containing silver (0) in a nanodispersed state, related to standard strains of several bacterial test cultures, showed a high antimicrobial activity. The inclusion of transition metal nanoparticles into HCFs has not been extensively studied.

The goal of the present study has been to use the solid matrix of a hydrate cellulose film for the synthesis of nickel nanospecies. To solve this, efficient methods were elaborated for the reduction of nickel ions in the HCF matrix by means of various reducers, to test the structure of the resulting cellulose-nickel composites, to determine the crystal phases of nickel, to identify nickel nano- and microparticles, to estimate their size distribution, and to establish whether these nanoparticles are stabilized in the matrix. Nanocomposite films based on hydrate cellulose and nickel are promising for the catalysis and preparation of magnetic and conducting materials.

## EXPERIMENTAL

### Materials and procedure

A hydrate cellulose film produced by Viscose Company (Russia) was used as a matrix for the intercalation of nickel species. Chemical modification of HCFs was carried out under heterogeneous conditions, *via* the diffusion-reduction method. The synthesis of nickel particles was performed by the reduction of metal ions from the aqueous solution of heptahydrate nickel sulfate  $\text{NiSO}_4 \cdot 7\text{H}_2\text{O}$  (Stavropol Plant of Chemical Reagents, Russia). Sodium tetrahydroborate  $\text{NaBH}_4$  (Ferak, Germany) and hypophosphite potassium  $\text{KH}_2\text{PO}_2 \cdot \text{H}_2\text{O}$  (Vekton, Russia) were used as reducers, and aqueous ammonia  $\text{NH}_3 \cdot \text{H}_2\text{O}$  (Reagent, Russia) was applied as an accessory agent. All reagents were of pure or analytical grade.

### Reduction of nickel ions with sodium tetrahydroborate

The HCF films were placed into a solution of  $\text{NiSO}_4 \cdot 7\text{H}_2\text{O}$  with a concentration of 0.135-0.350

mol/L, then kept at room temperature for 30 min. After diffusion, an aqueous NaBH<sub>4</sub> solution with a concentration of 0.015-1.450 mol/L was added under stirring. The duration of the reaction was 30 min. The molar ratio (MR) of the reducing agent ions (BH<sub>4</sub><sup>-</sup>) to metal ions (Ni<sup>2+</sup>) varied from 0.25 to 25. Further on, the HCF-Ni films were washed with distilled water and air-dried. The obtained films were coloured from dark grey to black, as depending on the MR.

#### Reduction of nickel ions with potassium hypophosphite

The HCF films were placed into a NiSO<sub>4</sub>·7H<sub>2</sub>O solution (concentration of 0.03-0.10 mol/L), together with an ammonia solution, which served as a pH regulator, and as a ligand of the nickel-ammonia complex [Ni(NH<sub>3</sub>)<sub>6</sub>]<sup>2+</sup>. The diffusion of nickel ions into the HCF bulk lasted for 30 min, after which a potassium hypophosphite solution with a concentration of 0.60-2.15 mol/L was added stepwise, the mixture being heated to 80 °C in a water bath and intensely stirred for 1 h. The MR of reducing agent ions (H<sub>2</sub>PO<sub>2</sub><sup>-</sup>) to metal ions (Ni<sup>2+</sup>) ranged<sup>22</sup> from 15 to 30. Then, the HCF-Ni films were washed and dried as previously described. The samples were grey-coloured, with different intensity.

#### Methods

The nickel concentration in bulk of the modified samples was determined by elemental analysis, using a Hewlett-Packard analyser.<sup>30</sup>

#### Wide Angle X-Ray Scattering (WAXS)

The structure of HCFs containing nickel was analysed by wide-angle X-ray scattering, on a DRON-2.0 diffractometer, using CuK<sub>α</sub> radiation. The X-ray scattering intensity curves were recorded<sup>19,20,22</sup> in the scattering angle range 5°<2θ<40°, with a 2θ/min angle step, and constant time of 3 s.

#### Scanning Electron Microscopy (SEM)

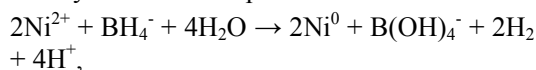
The morphological structure of the modified films was characterized by scanning electron microscopy on Stereoscan 360 (Cambridge, UK) and Jeol JSM-35 CF (Japan) electron microscopes. Measuring on Stereoscan 360 was accompanied by EDX analysis. The samples fixed on a carbon substrate in a special chamber were subjected to spraying in an inert atmosphere using a gold target. The capture by Jeol JSM-35 CF microscope was performed at 100-20000 magnifications and a voltage of 15 kW, on a Stereoscan 360 microscope – at a voltage of 20 kW. Histograms of the numerical distribution of nickel particles on the sample surface, according to their size, were obtained by the statistical processing of images

with a diameter referring to particle size. For each sample, at least 500 particles were analyzed.<sup>19,20,22</sup>

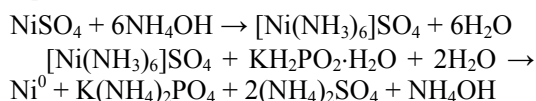
## RESULTS AND DISCUSSION

### Reduction of nickel ions and preparation of HCF-Ni nanocomposites

The reduction of nickel ions with sodium tetrahydroborate is represented as:<sup>31</sup>



while the formation of an ammonium complex of nickel and the reduction of nickel ions from a complex with potassium hypophosphite is represented as:<sup>31</sup>



When using NaBH<sub>4</sub>, the nickel content in the HCF-Ni samples greatly depends on the concentration of reducing agent and BH<sub>4</sub><sup>-</sup>/Ni<sup>2+</sup> molar ratio (Fig. 1). The dependence had an exponential shape. Reduction took place immediately, the maximum nickel content (8.6 wt%) achieving its limit at a BH<sub>4</sub><sup>-</sup>/Ni<sup>2+</sup> molar ratio equal to 4.0, and remaining unchanged when MR increased over 4.0. The reaction equation shows that, for a full reduction of the nickel ions, the MR BH<sub>4</sub><sup>-</sup>/Ni<sup>2+</sup> value should be lower than 4.0. Apparently, a considerable excess of MR was required, because the nickel ions diffused into the HCF pores were hard-to-reach for the reducing ions. With a further increasing MR, the reduction of Ni<sup>2+</sup> occurred mainly in a solution, resulting in nickel fall-out on the film surface, and in additional uses of the reducing agent.

When using KH<sub>2</sub>PO<sub>2</sub> as a reducer, the reaction took place at a H<sub>2</sub>PO<sub>2</sub><sup>-</sup>/Ni<sup>2+</sup> molar ratio above 20. It has been established experimentally that the optimum MR ratio was 25, which provided the maximum nickel content (10.0 wt%) in the samples. The 2.5 times increase in reducer concentration (from 0.7 to 1.7 mol/L) did not affect significantly the nickel content. Thus, the nickel content in the HCF-Ni sample depended on the reducer type and concentration.

#### WAXS study

The analysis of the X-ray scattering curves of the HCF-Ni samples (Figs. 2, 2 and 3) exhibited, besides the reflex in 2θ 20°, typical of HCF, some broad weak diffraction peaks at 2θ 45° and 51°, which referred to the reflection

from the planes 111 and 200 of crystalline nickel (0), respectively. Moreover, reflexes were occurred in position  $2\theta\ 36^\circ$ , related to the reflection from the plane 111 of the crystalline nickel oxide NiO.<sup>31,32</sup> However, in the X-ray scattering curves of the samples obtained by the reduction of nickel ions with NaBH<sub>4</sub>, the reflections corresponding to nickel (0) and its oxide proved to have a lower intensity than in the reduction with KH<sub>2</sub>PO<sub>2</sub>. This was due to the fact that, in the case of the reduction with NaBH<sub>4</sub>, the content of the reduced nickel was lower than in the case of KH<sub>2</sub>PO<sub>2</sub>. It should be also noted that, in contrast to the reduction with KH<sub>2</sub>PO<sub>2</sub>, the reflections corresponding to NiO in the case of NaBH<sub>4</sub> were comparable in size with the reflections corresponding to Ni(0). This indirectly indicated a higher content of the oxidized form of nickel in the case of NaBH<sub>4</sub>, which also agreed with the above data on the reduction having occurred mainly on the film surface. Consequently, finely reduced dispersed nickel (0), which was easily oxidized in air, was not stabilized by a HCF matrix, being oxidized to nickel oxide. Wide-angle X-ray scattering data also showed that the intercalation of nickel ions did not affect the supramolecular structure of HCF (Fig. 2, 1), as the structure of HCF-Ni composites corresponded to the structure of cellulose II.

### SEM study

The formation of Ni particles on the surface of HCF-Ni composite films has been evaluated

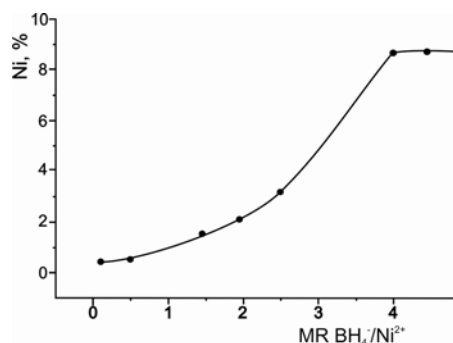


Figure 1: Dependence of nickel content on MR BH<sub>4</sub><sup>-</sup>/Ni<sup>2+</sup>

by SEM. Electron micrographs of HCFs containing nickel show that the reduction of nickel ions seems to have occurred differently, as depending on the type of the reducer. The use of NaBH<sub>4</sub> led mainly to the formation of solid nickel coatings consisting of spherical particles of nickel on both film surfaces (the latter was confirmed by EDX analysis). Nickel particles formed a cable-like chain structure on the surface, visible even at a slight zoom. Higher magnification showed that these chains consisted of laminated spherical particles of similar sizes (150-200 nm), which formed a sort of “beads” and/or large agglomerates in some parts (Fig. 3, 1). These structures, so-called “pearl necklace-like structures”, formed by transition metal species and imparting magnetic properties to nanocomposites, have been described in several publications.<sup>33-36</sup> They have been mainly received from solutions of polymers or inorganic matrices. In contrast to the mentioned studies, the structures obtained in the present investigation were first prepared *via* a heterogeneous process in the solid hydrate cellulose matrix.

Continuous coverage and chain structure of the nickel particles on the film surface were formed when the BH<sub>4</sub><sup>-</sup>/Ni<sup>2+</sup> MR was >4 in the reduction process. This confirmed the hypothesis that, at a higher concentration of reducing ions with respect to nickel ions, reduction took place mainly on the film surface, while the nickel species formed dense coatings that prevented embedding of nickel ions into the bulk of the film.

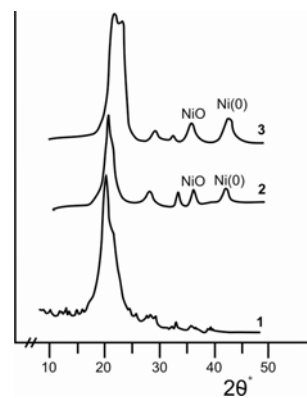


Figure 2: X-ray intensity curves of HCF (1); HCF-Ni, reducer NaBH<sub>4</sub>, Ni content = 4.9 wt% (2) HCF-Ni, reducer KH<sub>2</sub>PO<sub>2</sub>, Ni content = 10.0 wt% (3)

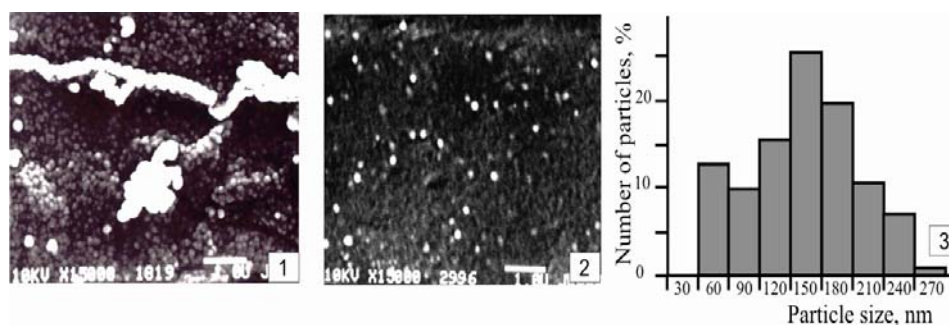


Figure 3: SEM images of HCF-Ni film surface prepared with reducer  $\text{NaBH}_4$ : films obtained at MR = 25, Ni content = 4.9 wt% (1); at MR = 0.25, Ni content = 0.6 wt% (2); and size distribution of nickel species in the sample prepared at MR = 0.25 (3)

When MC was  $<4$ , the pattern was different: the reduced nickel species were located discretely on the surface, and their sizes could be evaluated by the statistical analysis of micrographs (Fig. 3, 2). Nickel particles had diameter sizes from 30 to 250 nm, and the distribution of the largest number of particles was rather uniform in the 30-100 nm nanometer range (Fig. 3, 3). The particles were mostly spherical in shape, in contrast to the nickel particles described elsewhere.<sup>18,21,37</sup>

In contrast to the above results, the nickel particles obtained using  $\text{KH}_2\text{PO}_2$  had a quite larger size (Fig. 4, 1 and 2), the broad size distribution of the particles, consisting mainly of smaller species bundled into agglomerates, while the agglomerate size reached 5 mm. The formation of agglomerates was probably due to the electrostatic forces, which contributed to particle aggregation. The nickel species appeared not only on the film surface but also in the near-surface layer (Fig. 4, 2). This confirmed the results obtained in a previous study,<sup>23</sup> according to which, when treating HCF with solutions of the nickel-ammonia complex  $[\text{Ni}(\text{NH}_3)_n]^{2+}$ , which preceded the reduction of nickel ions, swelling of the film inner layers and increase in the interlayer spacing occurred. This resulted in the reduction of nickel ions not only on the film surface, but also in the bulk, and nickel species appeared everywhere. Nevertheless, the particles were strongly attached to the surface.

Thus, these results showed that, when using  $\text{NaBH}_4$  as a reducing agent, lower values of the reducer/metal ion MR were required to reach a nickel content of 8.9 wt%, while the size of most nickel species was in the nanoscale range. The samples obtained using  $\text{KH}_2\text{PO}_2$  had a higher nickel content (up to 10.0 wt%),

and both small (with nanometer-sized) and very large agglomerated particles were formed. However, some published results<sup>14,21</sup> showed that, when the nickel ions were reduced from the  $\text{NiCl}_2 \cdot 6\text{H}_2\text{O}$  solution with hydrazine hydrate in polymer matrices, the size of Ni(0) crystallites and species both on the surface and in the bulk did not essentially depend on the type of reducer used.

In contrast to such results, the authors found out that the reduction of nickel ions, the content of reduced nickel, nickel particle sizes and their distribution, as well as the stabilization of particles significantly depended on the morphological and structural features of the HCF matrix, and on the type of reducer, as well. Thus, when using  $\text{KH}_2\text{PO}_2$ , the film swelling contributed to the increase in the nickel content in HCF and to a partial intercalation of nickel into the bulk of the film. However, the necessity to maintain a high MR value during the reduction led to the agglomeration of nickel species on the surface of HCF, resulting in the particles with micrometer sizes. On the other hand, due to agglomeration, the oxidation of Ni(0) particles occurred to a lesser extent. When using  $\text{NaBH}_4$ , due to the high reaction rate, reduction occurred mainly on the film surface, and a continuous coating and cable-like structures appeared. In this case, particle sizes were much smaller and their oxidation on the surface increased.

The supramolecular structure of HCF, which had a lower crystallinity than microcrystalline cellulose,<sup>22,31,32</sup> did not significantly affect the intercalation of nickel species. The peculiar morphological structure of HCF plays the main role in nickel reduction. The morphology of the outer and inner layers

of the film was characterized as highly ordered, so that they had a certain barrier function. Consequently, the content of reduced nickel in HCF–Ni composites was lower than when using microcrystalline cellulose a matrix.<sup>22,31</sup>

Thus, the results of the present study showed that the HCF matrix could be successfully used to obtain nickel nano- and microspecies located mainly on the surface or

in the near-surface layer. A specific feature of nickel species synthesis and embedding into HCF was that the reduction and formation of nickel particles occurred under heterogeneous conditions in the solid matrix, which somehow limited the growth of species and, generally, the HCF behaviour in this reduction process could be evaluated as one of a neutral nanoreactor.

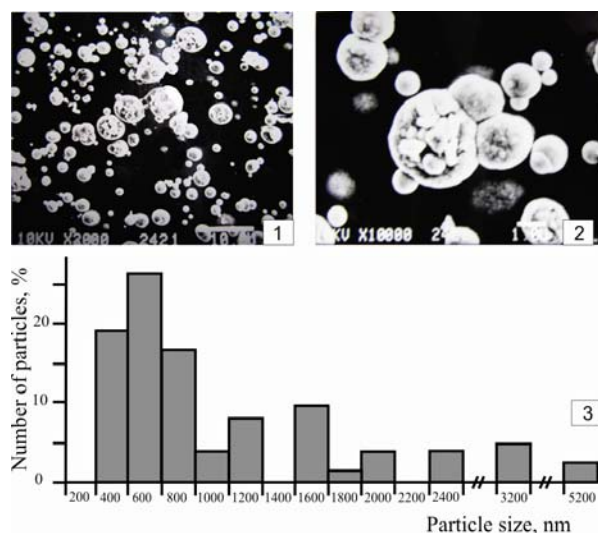


Figure 4: SEM micrographs of HCF–Ni film surface prepared with reducer  $\text{KH}_2\text{PO}_2$ : films with Ni content = 10.0 wt% (1, 2); size distribution of nickel species (3)

**ACKNOWLEDGEMENTS:** We are grateful to N. N. Saprikina for the SEM micrographs of the HCF–Ni samples, and to V. K. Lavrentiev for obtaining the X-ray intensity curves of the samples.

#### REFERENCES

- Yu. D. Tret'yakov, A. V. Lukashin and A. A. Eliseev, *Usp. Khim.*, **73**, 974 (2004).
- S. C. Davis, K. J. Klabunde and C. Stephen, *Chem. Rev.*, **82**, 153 (1982).
- A. R. St. Clair and L. T. Taylor, *J. Macromol. Sci., Chem.*, **16**, 95 (1981).
- A. B. Mayer and J. E. Mark, *J. Macromol. Sci., Pure Appl. Chem.*, **34**, 2151 (1997).
- S. P. Gubin and I. D. Kosobudskii, *Usp. Khim.*, **52**, 1350 (1983).
- W. Schulze and H. Abe, *Faraday Symp. Chem. Soc.*, **14**, 87 (1980).
- Yu. I. Petrov, "The Physics of Small Particles" (in Russian), Moscow, Nauka, 1982, 360 pp.
- S. P. Gubin, *Russ. Khim. Zh.*, **44**, 23 (2000).
- A. Sarkar, S. Kapoor, G. Yashwant *et al.*, *J. Phys. Chem., B*, **109**, 7203 (2005).

- K. M. Gorbunova, M. V. Ivanov and V. P. Moiseev, *J. Electrochem. Soc.*, **120**, 613 (1973).

- A. L. Volynskii and N. F. Bakeev, "Highly Dispersed Oriented State of Polymers" (in Russian), Moscow Khimiya, 1984, 192 pp.

- N. I. Nikonorova, E. V. Semenova, V. D. Zanegin *et al.*, *Polym. Sci., A*, **34**, 711 (1992), [*Vysokomol. Soedin., A*, **34**, 123 (1992)].

- S. V. Stakhanova, N. I. Nikonorova, A. L. Volynskii and N. F. Bakeev, *Polym. Sci., A*, **39**, 224 (1997), [*Vysokomol. Soedin., A*, **39**, 312 (1997)].

- I. M. Papisov, Yu. S. Yablokov, A. I. Prokof'ev and A. A. Litmanovich, *Polym. Sci., A*, **35**, 612 (1993), [*Vysokomol. Soedin., A*, **35**, 515 (1993)].

- I. M. Papisov, Yu. S. Yablokov and A. I. Prokof'ev, *Polym. Sci., A*, **36**, 291 (1994), [*Vysokomol. Soedin., A*, **36**, 352 (1994)].

- A. A. Litmanovich and I. M. Papisov, *Polym. Sci., B*, **39**, 41 (1997), [*Vysokomol. Soedin., B*, **39**, 323 (1997)].

- L. M. Bronshtein, P. M. Valetskii and M. Antonietti, *Polym. Sci., A*, **39**, 1249 (1997), [*Vysokomol. Soedin., A*, **39**, 1847 (1997)].

- <sup>18</sup> J. He, T. Kunitake and A. Nakao, *Chem. Mater.*, **15**, 4401 (2003).
- <sup>19</sup> N. E. Kotelnikova, G. Wegener, T. Paakkari *et al.*, *Zh. Obshch. Khim.*, **73**, 447 (2003).
- <sup>20</sup> N. E. Kotelnikova, G. Wegener, T. Paakkari *et al.*, *Cellulose Chem. Technol.*, **36**, 445 (2002).
- <sup>21</sup> J.-I. Ishiyama, T. Shirakawa, Y. Kurokawa and S. Imaizumi, *Angew. Makromol. Chem.*, **156**, 179 (1988).
- <sup>22</sup> N. E. Kotelnikova, E. L. Lysenko, R. Serimaa, K. Pirkkalainen, U. Vainio, V. K. Lavrent'ev, D. A. Medvedeva, A. L. Shakhmin, N. N. Saprykina and N. P. Novoselov, *Polym. Sci., A*, **50**, 51 (2008), [*Vysokomol. Soedin., A*, **50** (1), 63 (2008)].
- <sup>23</sup> N. E. Kotelnikova and A. M. Mikhailidi, *Cellulose Chem. Technol.*, **45**, 585 (2011).
- <sup>24</sup> E. Kontturi, T. Tammelin and M. Osterberg, *Chem. Soc. Rev.*, **35**, 1287 (2006).
- <sup>25</sup> E. Kontturi, P. C. Thune and J. W. H. Niemantsverdriet, *Langmuir*, **19**, 5735 (2003).
- <sup>26</sup> M. Koenig, V. Efferm, S. Redmann-Schmid and W. Lutz, US Patent 20080145576 (2008).
- <sup>27</sup> [http: polymers-money.com/journal/onlinejournal /2005/](http://polymers-money.com/journal/onlinejournal/2005/)
- <sup>28</sup> T. P. Starunskaya, *PhD Dissertation*, Leningrad, University, 1984, 142 pp.
- <sup>29</sup> N. E. Kotelnikova, O. V. Lashkevich and E. F. Panarin, Russian Patent 2256675 (2005).
- <sup>30</sup> V. A. Klimova, "The Main Micro-Analysis of Organic Compounds" (in Russian), Moscow, Khimia, 1975, 224 pp.
- <sup>31</sup> N. E. Kotelnikova, E. L. Lisenko, R. Serimaa, K. Pirkkalainen, U. Vainio, V. K. Lavrentiev, D. A. Medvedeva, A. L. Shakhmin, N. N. Saprikina and N. P. Novoselov, *Vysokomol. Soedin., A*, **49**, 1530 (2007).
- <sup>32</sup> K. Pirkkalainen, U. Vainio, K. Kisko, T. Elbra, T. Kohout, N. Kotelnikova and R. Serimaa, *J. Appl. Cryst.*, **40**, 489 (2007).
- <sup>33</sup> W. Zhou, L. He, R. Wang, K. Zheng, L. Guo, Ch. Chen, X. Han and Z. Zhang, *Nano Lett.*, **8**, 1147 (2008).
- <sup>34</sup> V. Salgueirino-Maceiraa, M. A. Correa-Duarte, A. Hucht and M. Farled, *J. Magn. Magn. Mater.*, **303**, 163 (2006).
- <sup>35</sup> Ya H. Zhang, F. Liang, N. Wang, L. Guo, L. He, Ch. Chen, Q. Zhang and Qu. Zhong, *J. Nanosci. Nanotechnol.*, **8**, 2057 (2008).
- <sup>36</sup> D. Kumar, S. J. Pennycook, A. Lupini, G. Duscher, A. Tiwari and J. Narayan, *Appl. Phys. Lett.*, **81**, 4204 (2002).
- <sup>37</sup> H. Wang, X. Kou, J. Zhang and J. Li, *Bull. Mater. Sci.*, **31**, 97 (2008).